

1  
2 **Water and Electrolyte Homeostasis in a Mouse Model with Reduced ENaC Gamma Subunit Expression**

3  
4 Evan C. Ray<sup>1</sup>, Alexa Jordahl<sup>1</sup>, Allison Marciszyn<sup>1</sup>, Aaliyah Winfrey<sup>1</sup>, Tracey Lam<sup>1</sup>, Yaacov Barak<sup>2</sup>, Shaohu  
5 Sheng<sup>1</sup>, and Thomas R. Kleyman<sup>1,3,4</sup>.

6  
7 Departments of <sup>1</sup>Medicine, <sup>2</sup>Obstetrics, Gynecology & Reproductive Sciences, <sup>3</sup>Cell Biology, and  
8 <sup>4</sup>Pharmacology and Chemical Biology, University of Pittsburgh; and; <sup>2</sup>Magee-Womens Research Institute,  
9 Pittsburgh, PA.

10  
11 Running Title: Mouse with Reduced ENaC Gamma Subunit Expression

12  
13 Keywords: ENaC, Potassium Excretion, Salt Sensitivity, Extracellular Fluid Volume, Quantitative magnetic  
14 resonance

15  
16 Address all correspondence to:

17  
18 Evan C. Ray, MD PhD  
19 Renal-Electrolyte Division  
20 University of Pittsburgh  
21 A919 Scaife Hall,  
22 3550 Terrace Street  
23 Pittsburgh, PA 15261  
24 Email: rayec@upmc.edu

25  
26  
27  
28

29 **Abstract**

30

31 The epithelial Na<sup>+</sup> channel (ENaC) promotes the absorption of Na<sup>+</sup> in the aldosterone-sensitive distal  
32 nephron, colon, and respiratory epithelia. Deletion of genes encoding ENaC's subunits results in early  
33 post-natal mortality. We present initial characterization of a mouse with dramatically suppressed  
34 expression of the  $\gamma$  subunit. We use this hypomorphic ( $\gamma^{mt}$ ) allele to explore the importance of ENaC's  $\gamma$   
35 subunit in homeostasis of electrolytes and body fluid volume. At baseline,  $\gamma$  subunit expression in  $\gamma^{mt/mt}$   
36 mice is markedly suppressed in kidney and lung, while electrolytes resemble those of littermate  
37 controls. Challenge with a high K<sup>+</sup> diet does not cause significant differences in blood K<sup>+</sup>, but provokes  
38 higher aldosterone in  $\gamma^{mt/mt}$  mice than controls. Quantitative magnetic resonance (QMR) measurement  
39 of body composition reveals similar baseline body water, lean tissue mass, and fat tissue mass in  $\gamma^{mt/mt}$   
40 mice and controls. Surprisingly, euvoemia is sustained without significant changes in aldosterone or  
41 atrial natriuretic peptide.  $\gamma^{mt/mt}$  mice exhibit a more rapid decline in body water and lean tissue mass in  
42 response to a low Na<sup>+</sup> diet than controls. Replacement of drinking water with 2% saline induces  
43 dramatic increases in body fat in both genotypes, and a selective transient increase in body water and  
44 lean tissue mass in  $\gamma^{mt/mt}$  mice. While ENaC in renal tubules and colon work to prevent extracellular fluid  
45 volume depletion, our observations suggest that ENaC in non-epithelial tissues may have a role in  
46 preventing extracellular fluid volume overload.

47

48

49

## 50 **Introduction**

51 The epithelial Na<sup>+</sup> channel (ENaC) has a key role in regulation of extracellular fluid volume and blood  
52 pressure, and renal K<sup>+</sup> secretion. ENaC loss of function mutations in humans cause  
53 pseudohypoaldosteronism type 1 (PHA1), associated with urinary Na<sup>+</sup> wasting, polyuria, hypotension,  
54 hyperkalemia and elevated aldosterone, reflecting extracellular fluid volume contraction (37). Gain-of-  
55 function mutations cause Liddle syndrome, characterized by hypertension, suppressed aldosterone, and  
56 hypokalemia secondary to enhanced renal tubular Na<sup>+</sup> absorption and K<sup>+</sup> secretion (37). The importance  
57 of ENaC in regulating Na<sup>+</sup> handling and extracellular fluid volume suggest that ENaC activity may play a  
58 role in salt-sensitive hypertension (16, 25, 28).

59 The essential nature of the genes encoding ENaC's subunits,  $\alpha$ ,  $\beta$ , or  $\gamma$ , has impaired investigation of the  
60 functional contributions of these subunits. A hypomorphic  $\beta$  subunit allele has proven useful in assessing  
61 the physiologic importance of this subunit, though complicated by inclusion of a Liddle syndrome  
62 mutation in the hypomorphic  $\beta$  subunit allele (29). Mice expressing this allele demonstrate more than  
63 twenty-fold reduction in  $\beta$  subunit expression but survive to adulthood, exhibiting a PHA1-like  
64 phenotype. Subsequent studies capitalized on this useful genetic tool to demonstrate the importance of  
65 the  $\beta$  subunit in modulation of respiratory fluid clearance, arterial myogenic vasoconstriction, renal  
66 vascular blood flow, and baroreception (9, 11, 14, 31).

67 Here, we present initial characterization of a gene-targeted mouse strain expressing a hypomorphic  $\gamma$   
68 subunit allele, resulting in dramatically reduced expression in both kidney and lung but supporting  
69 viability in the homozygous state ( $\gamma^{mt/mt}$ ). This hypomorphic allele allows exploration of the importance  
70 of ENaC's  $\gamma$  subunit in homeostasis of electrolytes and body fluid volume.

## 71 **Methods**

72 *Generation and care of  $\gamma$  subunit hypomorphic mice:* Gene-targeted mice were produced using  
73 homologous recombination in embryonic stem (ES) cells. *Scnn1g* exon 2 and 7 to 8 kB of flanking DNA  
74 were cloned from a Chromosome 7 bacterial artificial chromosome (BACPAC Genomics). The cDNA for  
75 the only known transcript of *Scnn1g* was inserted, in frame, distal to the start codon in *Scnn1g* exon 2  
76 (Figure 1). An accompanying neomycin cassette decreased expression of the targeted locus. (27)  
77 Embryonic stem cells were electroporated with this construct. Correct insertion of the transgene was  
78 confirmed in G418-resistant stem cells by Southern blot. Chimeric mice carrying the targeted allele  
79 were produced at Charles River Inc. by microinjection of blastocysts with correctly targeted ES cell  
80 clones. Male progeny with germline incorporation of the transgene were selected as founders of  
81 independent mouse lines. Progeny were back-crossed for four to five generations into the  
82 129S2/SvPasCrl (129sv, Charles River) or C57B/6 (Jackson Labs) background. Heterozygous ( $\gamma^{+/mt}$ ) mice  
83 from the two separate lines were cross-bred to generate experimental mice and littermate controls.  
84 Genotyping was performed in a single reaction with the following three primers: pER31 (intron 1  
85 common forward primer: ACC TTA CTT GGC TCC TCT GTC CCT TC), pER32 (transgenic exon 2-3 junction  
86 reverse primer: GGA GGT CAC TCA CAG CAC TGT ACT TGT AG), and pER35 (wild-type intron 2 reverse  
87 primer: GGA GGC AGA TGC TAA CCT CAT TTC AGG). Amplification products were 633 bp ( $\gamma^{+}$ ) and 400 bp  
88 ( $\gamma^{mt}$ ). All control mice were littermates of  $\gamma^{mt/mt}$  mice.

89 Regular diet included 0.94% K<sup>+</sup> and 0.23% Na<sup>+</sup> (Prolab Isopro RMH 3000, LabDiet). High K<sup>+</sup> diet contained  
90 5.2% K<sup>+</sup> (as KCl) and 0.3% Na<sup>+</sup> (Teklad TD.09075, Envigo). Low Na<sup>+</sup> diet (TD.90228) contained 0.01-0.02%  
91 Na<sup>+</sup> and 0.8% K<sup>+</sup>. 2% saline was unbuffered 2 g/dL NaCl in dH<sub>2</sub>O (w/v). All animal work was approved by  
92 University of Pittsburgh Institutional Animal Care and Use Committee.

93 *Measurement of electrolytes and hormones:* Whole blood was collected upon mouse sacrifice via  
94 aspiration from a cardiac ventricle and measurements were performed immediately using an iSTAT

95 handheld device (Abbott Point of Care, Inc.). ELISAs for aldosterone (Enzo Life Sciences, catalog number  
96 ADI-900-173) or ANP (Sigma-Aldrich catalog number RAB00385) were performed on plasma diluted 1:25  
97 to 1:200 or 1:4, respectively.

98 *Immunoblotting:* Tissues were stored at -80 degrees C° until use. Approximately 50 mg of tissue was  
99 homogenized using a Dounce homogenizer in 0.15 mL (for kidney) or 0.2 mL (for lung) HEPES-buffered  
100 saline plus Phosphatase Inhibitor Cocktail Set II and Protease Inhibitor Cocktail Set III (Calbiochem).  
101 Protein was measured using a Pierce™ BCA protein assay kit (Thermo Fisher) and mixed 1:1 with 2x  
102 Laemmli buffer (Bio-Rad) plus 5% β-mercaptoethanol. Sixty µg of protein were loaded per well in a 4-  
103 15% acrylamide TGX gel (Bio-Rad) and run in 1x Tris-Glycine SDS buffer. Proteins were transferred to  
104 nitrocellulose, and blocked in 10% milk in TBST. Primary antibodies included anti-γ subunit (StressMarq;  
105 catalogue number SPC-405; 0.5 µg/mL), anti-β subunit (StressMarq; catalogue number SMC-241; 1  
106 µg/mL), and anti-GAPDH (ProteinTech, 0.1 µg/mL). After incubation with appropriate HRP-linked  
107 secondary antibodies, blots were digitally analyzed a ChemiDoc Imaging System (Bio-Rad).

108 *Body composition analysis:* *In vivo* mouse body composition was measured by quantitative magnetic  
109 resonance using a 100H Body Composition Analyzer (EchoMRI™)(40, 43). QMR was recently shown to be  
110 effective at detecting progressive differences in body water in response to changes in dietary Na<sup>+</sup> and  
111 water or mineralocorticoid treatment (24). Measurements were performed **in** late afternoon. Tag-free,  
112 un-anesthetized, ~10 week-old mice were weighed, immediately placed in a restraint tube (EchoMRI),  
113 and inserted into the analyzer. The tube was carefully examined to ensure absence of urine or other  
114 fluid from previously measured mice. Choice of restraint tube influenced measurements, therefore the  
115 same tube was used for all measurements. Each measurement required less than 3 minutes. After  
116 measurement, each mouse was returned immediately to its cage. After all mice were measured once,  
117 the all mice were individually weighed and measured again. Data shown represent mean of two

118 measurements. Mouse weights and body water declined by 0.2 to 0.6 g between measurements (~1  
119 hour apart), so mice were measured in the same order each session.

120 *Statistics:* Outliers were removed using the ROUT method (ROUT coefficient of 1%). Pair-wise  
121 comparisons were performed by Student's *t*-test ( $\alpha = 0.05$ ). For multiple, independent comparisons, *p*  
122 was adjusted using Sidak's method (38). For non-independent, repeated measurements (body  
123 composition over time), false discovery rates were controlled using Benjamini, Krieger, and Yekutieli's  
124 two-stage step-up method ( $Q = 0.05$ ), and *p* values adjusted accordingly (3). Analyses were performed  
125 using Prism 8.4.2 (GraphPad). Reported errors represent standard deviation.

## 126 RESULTS

127 Immunoblots of whole kidneys and lungs from transgenic mice ( $\gamma^{\text{mt/mt}}$ ) and littermate controls ( $\gamma^{+/+}$ )  
128 revealed reduced  $\gamma$  subunit expression (Figure 2). In kidney,  $\gamma$  subunit (normalized to  $\gamma^{+/+}$ ) was reduced  
129 from  $100 \pm 10\%$  ( $N = 5$ ) to  $8 \pm 4\%$  ( $N = 6$ ;  $p < 0.0001$ ). In lung, it was reduced from  $100 \pm 43\%$  ( $N = 6$ ) to  
130  $16 \pm 4\%$  ( $N = 4$ ;  $p < 0.01$ ).  $\beta$  subunit expression was not significantly different:  $100 \pm 60\%$  ( $N = 5$ ) in  
131 control kidneys versus  $62 \pm 21\%$  ( $N = 6$ ,  $p = \text{NS}$ ) in  $\gamma^{\text{mt/mt}}$  kidneys, and  $100 \pm 49\%$  ( $N = 6$ ) in control lungs  
132 versus  $144\% \pm 132\%$  ( $N = 5$ ) in  $\gamma^{\text{mt/mt}}$  lungs ( $p = \text{NS}$ ).

133 Because deletions of ENaC subunits exhibit early post-natal mortality, we examined litter size and  
134 genotype ratios in  $\gamma^{+/mt}$  crosses. (2) Litter size at weaning was  $4.4 \pm 1.8$  for 129sv pups (25 litters) and  $5.2$   
135  $\pm 1.9$  for C57BL/6 pups (5 litters). These resemble previously reported wild-type litter sizes of 4.6 for  
136 129sv mice and 5.5 for C57BL/6 mice (12). Analysis of litters from 23 heterozygote crosses in the 129sv  
137 background revealed that live  $\gamma^{\text{mt/mt}}$  pups were present at near-Mendelian ratios (29 out of 103  
138 compared to 28/103 and 46/103 for  $\gamma^{+/+}$  and  $\gamma^{+/mt}$  pups, respectively). Weights of  $\gamma^{\text{mt/mt}}$  mice resembled

139 age- and sex-matched controls. These data indicate no significant pre- or peri-natal mortality or  
140 abnormal growth of  $\gamma^{mt/mt}$  mice.

141 Pharmacologic or genetic inhibition of ENaC causes hyperkalemia (2, 32, 44). On a regular diet, blood  $K^+$ ,  
142  $Na^+$ ,  $Cl^-$ , total  $CO_2$  ( $tCO_2$ ), urea nitrogen (BUN), and hemoglobin (Hb) from  $\gamma^{mt/mt}$  mice resembled controls  
143 (Table 1 and Figure 4). Measurements in 129sv mice resembled C57B6/J mice. Blood  $K^+$  also did not  
144 differ between genotypes on a high  $K^+$  diet (Table 2 and Figure 5). The point-estimate for blood  $K^+$  in  
145  $\gamma^{mt/mt}$  males exceeded that of  $\gamma^{+/+}$  males, but did not reach significance (adjusted  $p = 0.09$ ). Blood  $Na^+$  was  
146 lower in  $\gamma^{mt/mt}$  females than in  $\gamma^{+/+}$  females (adjusted  $p = 0.04$ ).

147 Increased blood  $K^+$  stimulates aldosterone secretion, as does decreased blood volume. Either of these  
148 could increase aldosterone in the plasma of  $\gamma^{mt/mt}$  mice. Elevated aldosterone enhances urinary  $K^+$   
149 excretion and would attenuate any increase in blood  $K^+$  in  $\gamma^{mt/mt}$  mice. On a regular diet, plasma  
150 aldosterone from  $\gamma^{mt/mt}$  mice were similar to those of  $\gamma^{+/+}$  mice ( $\gamma^{+/+}$ :  $580 \pm 720$  pg/mL,  $N = 11$ ;  $\gamma^{mt/mt}$ :  $880$   
151  $\pm 610$ ,  $N = 9$ ,  $p = NS$ ) Atrial natriuretic peptide (ANP) levels were also similar between groups (Table 1).  
152 Mean plasma aldosterone levels increased in both  $\gamma^{mt/mt}$  and  $\gamma^{+/+}$  mice when mice were placed on a high  
153  $K^+$  diet for 10 days, but they were higher in  $\gamma^{mt/mt}$  mice than in controls (Figure 6 and Table 2;  $\gamma^{+/+}$   $3100 \pm$   
154  $2500$  pg/mL,  $N = 19$ ;  $\gamma^{mt/mt}$   $4900 \pm 2500$ ,  $N = 23$ ,  $p < 0.05$ ). This difference was not evident when males  
155 and females were analyzed separately.

156 We hypothesized that  $\gamma^{mt/mt}$  mice would exhibit similar total body water and lean tissue mass when  
157 compared against  $\gamma^{+/+}$  littermates on a regular diet, given that plasma aldosterone and ANP levels were  
158 similar. Quantitative magnetic resonance revealed no significant differences in percent body water, lean  
159 tissue mass, or fat tissue mass (Figure 7). For  $\gamma^{+/+}$  mice, body water was  $67.7 \pm 2.7$  % ( $N = 10$ ; 1 female  
160 and 9 males), compared to  $67.4 \pm 2.6$  % for  $\gamma^{mt/mt}$  mice ( $N = 7$ ; 2 female and 5 males;  $p = NS$ ). Lean tissue

161 mass was  $79.9 \pm 2.5$  % vs.  $79.4 \pm 3.0$  % ( $p = \text{NS}$ ), and fat composition was  $12.0 \pm 3.1$  % vs.  $12.8 \pm 3.1$  % ( $p$   
162 = NS).

163  $\gamma^{\text{mt/mt}}$  mice did not have evidence of volume depletion at baseline. To evaluate whether compensatory  
164 mechanisms could be overcome by physiologic stress, animals were given a  $\text{Na}^+$ -depleted (0.01-0.02%  
165  $\text{Na}^+$ ) diet (Figure 7). Over six days, body weights decreased significantly overall ( $p < 0.0001$ ). However,  
166 genotype-dependent differences in body weight were not observed. Similarly, normalized body water  
167 percentage decreased over this period ( $P < 0.0001$ ). The  $\gamma^{\text{mt/mt}}$  mice exhibited lower normalized body  
168 water at day 2 than controls ( $99.1 \pm 2.1\%$  for  $\gamma^{+/+}$  mice,  $N = 10$ ;  $96.3 \pm 2.7$  % for  $\gamma^{\text{mt/mt}}$  mice,  $N = 7$ ;  
169 adjusted  $p = 0.03$ ; Figure 7). Subsequently, differences between genotypes lost significance. Normalized  
170 lean tissue mass also decreased overall ( $p = 0.002$ ). At day 2,  $\gamma^{\text{mt/mt}}$  mice exhibited lower normalized lean  
171 mass than controls ( $100.3 \pm 2.1\%$  for  $\gamma^{+/+}$  mice,  $N = 10$ ;  $97.1 \pm 1.9$  % for  $\gamma^{\text{mt/mt}}$  mice,  $N = 7$ ; adjusted  $p <$   
172  $0.01$ ). Body fat did not change in either group.

173 The ability of ENaC to promote renal and gastrointestinal  $\text{Na}^+$  retention has led to the hypothesis that  
174 the channel may contribute to salt-sensitive hypertension (16, 34, 35). We therefore asked whether  
175  $\gamma^{\text{mt/mt}}$  mice were protected from fluid volume overload during an obligatory increase in  $\text{Na}^+$  intake  
176 associated with replacement of electrolyte-free drinking water with 2% saline. Mice prefer saline to  
177 electrolyte-free water and consume more than 6 mL of 2% saline per day (19). The saline increased body  
178 weights significantly by 9 days, with no difference between groups ( $106 \pm 6.8$  %,  $N = 10$   $\gamma^{+/+}$  mice and  $107$   
179  $\pm 4.2$  %,  $N = 7$   $\gamma^{\text{mt/mt}}$  mice, on day 9,  $p = \text{NS}$ ; Figure 7). Body water increased in  $\gamma^{\text{mt/mt}}$  mice relative to  
180 controls at day two (to  $101.7 \pm 2.1\%$  vs.  $98.9 \pm 2.6\%$ , respectively; adjusted  $p = 0.03$ ).  $\gamma^{\text{mt/mt}}$  mice also  
181 exhibited higher lean tissue mass on day two ( $101.9 \pm 1.7\%$  vs.  $99.1 \pm 1.7\%$ , respectively;  $p = 0.04$ ). Body  
182 water and lean tissue masses did not differ significantly on later days. Body fat increased dramatically,  
183 but similarly, in  $\gamma^{+/+}$  and  $\gamma^{\text{mt/mt}}$  mice over 9 days (to  $140.7 \pm 30.7$  % and  $149.7 \pm 28.3$  %, respectively).



184 **Discussion**

185 These results demonstrate a grossly healthy mouse model with reduced expression of ENaC's  $\gamma$  subunit.  
186 Homozygous mice have no evidence of volume-depletion or impaired  $K^+$  handling at baseline, but exhibit  
187 aldosterone on a high  $K^+$  diet suggesting impaired  $K^+$  secretion. They experience enhanced sensitivity of  
188 body fluid volume to changes in dietary  $Na^+$ , with more rapid loss of fluid and lean tissue on a low  $Na^+$   
189 diet. Surprisingly, a transient larger increase in fluid and lean tissue mass was observed when water was  
190 replaced with 2% saline to drink. A dramatic increase in body fat content occurs in both  $\gamma^{mt/mt}$  and  $\gamma^{+/+}$   
191 mice given 2% saline. Finally, these studies illustrate the utility of quantitative magnetic resonance in  
192 assessing fluid volume in dietary and genetic mouse models.

193  $\gamma^{mt/mt}$  mice should prove valuable for further investigations into the physiologic role of ENaC's  $\gamma$  subunit,  
194 an essential protein. Floxed models allow targeted deletion in specific tissues, but depend upon  
195 available Cre-expressing mouse lines (21, 36). A  $\beta$  subunit hypomorph with a  $\beta$  subunit Liddle syndrome  
196 variant has previously been reported (29, 39). The contribution of different subunits to the physiology of  
197 various cell-types likely differs, and this mouse will facilitate investigation of the physiologic role of the  $\gamma$   
198 subunit.

199 The  $\gamma^{mt/mt}$  mice exhibit significantly higher aldosterone on a high  $K^+$  diet, suggesting impaired  $K^+$   
200 secretion. In the aldosterone-sensitive distal nephron, ENaC-mediated  $Na^+$  reabsorption is tightly linked  
201 to  $K^+$  excretion. Pharmacologic or genetic impairment of ENaC activity reduce  $K^+$  secretion and promote  
202 hyperkalemia (4, 6). It is therefore surprising that  $\gamma^{mt/mt}$  mice exhibit blood  $K^+$  levels similar to controls.  
203 On a high  $K^+$  diet, the renal tubule increases  $K^+$  secretion through pathways that are both ENaC-  
204 dependent and ENaC-independent (13). This adaptation includes up-regulation of ROMK channels in  
205 principal cells, and BK channels in intercalated cells (7, 33). The  $\gamma^{mt/mt}$  mice may compensate for impaired  
206 ENaC-dependent  $K^+$  secretion by upregulating alternative  $K^+$  secretory pathways.

207 The  $\gamma^{mt/mt}$  animals exhibit no evidence of body fluid depletion at baseline, as indicated by: i) aldosterone  
208 and ANP levels that are indistinguishable from controls; ii) hemoglobin levels that reveal no signs of  
209 hemoconcentration; iii) BUN levels that are not elevated; and iv) body water and lean tissue mass that  
210 do not differ from controls. These findings stand in contrast to the induced  $\gamma$  subunit knock-out in the  
211 kidney of adult mice, which causes weight loss, hemoconcentration, and elevated aldosterone (5).  
212 Residual ENaC activity likely contributes, but additional compensatory mechanisms are likely. A  
213 downregulation of ENaC in non-epithelial sites (see below) might also contribute.

214 Dietary  $\text{Na}^+$  restriction produces a more rapid decline in body water and lean tissue in  $\gamma^{mt/mt}$  mice than in  
215 controls. More surprising is the response of  $\gamma^{mt/mt}$  mice given saline as drinking fluid. We predicted that  
216 impaired enteric and renal  $\text{Na}^+$  absorption would attenuate increases in body water associated with  
217 increased  $\text{Na}^+$  consumption. Instead, saline causes a significant, transient increase in total body fluid in  
218  $\gamma^{mt/mt}$  animals but not controls. If confirmed, these findings may point to a role for ENaC's  $\gamma$  subunit not  
219 only in promoting  $\text{Na}^+$  retention in the context of dietary  $\text{Na}^+$  depletion, but also in preventing volume-  
220 overload in the context of increased  $\text{Na}^+$  consumption.

221 Such a role may depend upon the function of ENaC in tissues beyond the kidney tubule. One group  
222 observed that global  $\beta$  subunit suppression increases blood pressure, as measured with intravascular  
223 telemetry catheters (9). Another group found no change in blood pressure, although they measured  
224 blood pressures in anesthetized mice using physically coupled catheters (29). Increased blood pressure  
225 and our finding of increased fluid volume sensitivity to dietary saline might reflect ENaC activity in extra-  
226 epithelial tissues where the channel is expressed, such as arterial baroreceptors, vascular endothelium  
227 and myocytes, dendritic cells, or central nervous system osmosensors (8, 10, 23, 41). Providing mice  
228 with saline to drink increases  $\text{Na}^+$  consumption, but also deprives them of electrolyte-free water. Further

229 studies will be required to confirm these findings and to determine whether they are the result of fluid  
230 volume overload or relative water deprivation and increased serum tonicity.

231 A recent report demonstrated increased lipolysis in the context of replacement of drinking water with  
232 2% saline (20, 30). The authors observed increased fat catabolism when dietary calorie in-take was fixed.  
233 However, the authors also noted that mice given 2% saline to drink and *ad libitum* food experience  
234 weight gain (20). As our mice were also provided food *ad libitum*, our observations are consistent with  
235 the previously reported increase in body weight, and show that the increase in weight with 2% saline  
236 specifically reflects an increase in fat mass. This illustrates an important caveat relating to the conclusion  
237 that increased salt intake stimulates lipolysis. Fat break-down may only occur when increased calorie  
238 consumption is prevented.

239 Finally, this study illustrates the usefulness of quantitative magnetic resonance (QMR) in evaluating  
240 body fluid content in genetic mouse models. Though percent changes in total body water were small,  
241 they likely under-represent change in extracellular water, which contributes only 1/3 of total body water  
242 (15). QMR has been used extensively for evaluation of body-fat content, but a recent study showed  
243 changes in body water due water deprivation or aldosterone administration (24). The appeal of this  
244 method stems from the ability to perform repeated measures in live, unanesthetized animals.  
245 Measurements detect changes not detectable by weight alone.

246 The findings in this manuscript demonstrate a novel genetic tool for exploring the importance of ENaC's  
247  $\gamma$  subunit *in vivo*. These findings, if confirmed, would suggest a surprising role for ENaC in salt-  
248 sensitivity, protecting against changes in body volume due to acute dietary increases in  $\text{Na}^+$   
249 consumption.

250 **Acknowledgments**

251 This work was supported by grants from the National institutes of Health, including K08 DK110332, R01  
252 HL147818, T32 DK061296 and P30 DK079307.

253

## 254 **Figure Legends**

255 **Figure 1. Generation of an *Scnn1g* Hypomorphic Allele.** A schematic of the wild-type and transgenic  
256 *Scnn1g* locus (encoding the ENaC  $\gamma$  subunit) is shown in **A**. The genomic region corresponding to the  
257 targeting construct is represented as a hatched box. Open, boxes represent exons. Gray bars (with \*)  
258 represent radiolabeled probes used for Southern blot. These are external to the targeting construct.  
259 Neo: neomycin-resistance cassette.  $\gamma$  ENaC-V5: cDNA for ENaC's  $\gamma$  subunit, with C-terminal V5 tag, driven  
260 in frame by the start codon of the native gene. Restriction sites used for Southern blot are marked. **B**.  
261 Homologous recombination of the 5' arm was analyzed by Southern blot of *SacI*-digested ES cell  
262 genomic DNA with the 5' probe (not shown). Shown is a Southern blot with the 3' probe of *NdeI*-  
263 digested genomic DNA of three representative clones from the 5' analysis, confirming homologous  
264 recombination of the 3' arm, which manifests as a shift in the size of the probed fragment from 8.0 to  
265 12.6 kb. +: clones with correct homologous recombination of the 3' arm. M: KB markers.

266 **Figure 2.  $\gamma^{mt/mt}$  mice express significantly less  $\gamma$  subunit in kidney and lung.** Immunoblots of kidney and  
267 lung tissue lysates were probed with antibodies against the  $\beta$  or  $\gamma$  subunit of ENaC, then stripped and  
268 probed with antibodies against GAPDH. Arrowheads on the left of each blot show molecular weight  
269 marker positions. Carrots on the right of each blot indicate approximate region taken for signal  
270 quantification. Dot plots show protein normalized to mean signal from  $\gamma^{+/+}$  mice. Squares represent  
271 males, circles represent females. Open or shaded symbols represent data from 129sv or C57BL/6 mice,  
272 respectively.  $\gamma$  subunit protein levels in  $\gamma^{mt/mt}$  mouse kidneys were reduced from  $100 \pm 10$  % (mean  $\pm$  SD,  
273 N = 5 mice) to  $8 \pm 4$  % (N = 6). \*\*\*:  $p < 0.0001$  (two-tailed Student's t-test). In lung, the  $\gamma$  subunit was

274 reduced from  $100 \pm 43\%$  (N = 6) to  $16 \pm 4\%$  (N = 4) \*\*:  $p < 0.01$  (two-tailed Student's t-test). The kidney  
275  $\beta$  subunit point estimate decreased from  $100 \pm 60\%$  (N = 6) to  $62 \pm 9\%$  (N = 6), but the difference was  
276 not significant. Lung  $\beta$  subunit protein signal also did not differ significantly between groups:  $100 \pm 49\%$   
277 (N = 6) for  $\gamma^{+/+}$  vs.  $144 \pm 132\%$  for  $\gamma^{mt/mt}$  (N = 5).

278 **Figure 3. Pups born to  $\gamma^{+/mt}$  parents exhibit genotype frequencies consistent with Mendelian**  
279 **inheritance and gain weight normally.** Left and right plots demonstrate that  $\gamma^{mt/mt}$  mice exhibit weights  
280 similar to age- and sex-matched  $\gamma^{+/+}$  littermate controls. 8 to 10 week-old mice:  $\gamma^{+/+}$  males weighed  $26.0$   
281  $\pm 0.9$  g, N = 5;  $\gamma^{mt/mt}$  males weighed  $27.1 \pm 0.9$  g, N = 4,  $p = \text{NS}$ .  $\gamma^{+/+}$  females weighed  $21.1 \pm 0.4$  g, N = 7;  
282  $\gamma^{mt/mt}$  females weighed  $21.0 \pm 0.8$  g, N = 3,  $p = \text{NS}$ . 22 to 24 week-old mice:  $\gamma^{+/+}$  males weighed  $34.4 \pm 6.1$   
283 g, N = 3;  $\gamma^{mt/mt}$  males weighed  $33.3 \pm 3.3$  g, N = 3,  $p = \text{NS}$ ;  $\gamma^{+/+}$  females weighed  $26.7 \pm 2.3$  g, N = 3;  $\gamma^{mt/mt}$   
284 females weighed  $25.35 \pm 2.2$  g, N = 4,  $p = \text{NS}$ . (Comparisons examined using two-tailed Student's t-test.)  
285 Open or shaded symbols represent data from 129sv or C57BL/6 mice, respectively.

286 **Figure 4. Blood analytes are similar in  $\gamma^{mt/mt}$  and  $\gamma^{+/+}$  mice.** Blood parameters from mice on a regular  
287 diet are shown. Electrolytes, urea nitrogen, hemoglobin, and creatinine were measured in whole blood.  
288 Open symbols represent mice in the 129sv background; shaded symbols represent the C57BL/6  
289 background. There were no significant differences between  $\gamma^{+/+}$  mice and  $\gamma^{mt/mt}$  mice, as determined by  
290 two-tailed Student's t-test with adjustment of  $p$  values for multiple comparisons (two sexes) using  
291 Sidak's method. Please see Table 1 for means and standard deviations.

292 **Figure 5. On a high  $K^+$  diet, blood electrolyte, BUN and Hb concentrations in  $\gamma^{mt/mt}$  mice largely**  
293 **resemble those of  $\gamma^{+/+}$  mice.** 129sv mice were provided with 5.2%  $K^+$  (as KCl) diet for 10 days before  
294 blood collection. Electrolytes, urea nitrogen, hemoglobin, and creatinine were measured in whole blood.  
295 Blood  $Na^+$  was higher in female  $\gamma^{+/+}$  mice than in  $\gamma^{mt/mt}$  mice ( $146 \pm 2$ , N = 9 vs.  $144 \pm 2$ , N = 7; adjusted  $p$

296 = < 0.05). There were no other significant differences between  $\gamma^{+/+}$  mice and  $\gamma^{mt/mt}$  mice. Groups were  
297 compared using two-tailed Student's t-test with adjustment of  $p$  values for multiple comparisons in two  
298 sexes using Sidak's method. See Table 2 for means and standard deviations.

299 **Figure 6. Plasma aldosterone levels in  $\gamma^{mt/mt}$  mice are similar to controls at baseline, but are higher**  
300 **than  $\gamma^{+/+}$  littermate controls on a high  $K^+$  diet.** 129sv mice were maintained on a regular (0.94%  $K^+$ ) diet,  
301 or transitioned to a 5.2%  $K^+$  (as KCl) diet for 10 days. Squares represent males, circles represent females.  
302 On a regular diet, there was no differences in plasma aldosterone between  $\gamma^{+/+}$  mice ( $590 \pm 720$  pg/mL,  
303  $N = 11$ ) and  $\gamma^{mt/mt}$  mice ( $880 \pm 610$  pg/mL,  $N = 9$ ). On the high  $K^+$  diet, aldosterone increased in both  
304 groups (to  $3100 \pm 2500$  pg/mL,  $N = 19$  in  $\gamma^{+/+}$  mice, adjusted  $p < 0.05$  compared to  $\gamma^{+/+}$  mice on a regular  
305 diet; and  $4900 \pm 2500$  pg/mL,  $N = 23$  in  $\gamma^{mt/mt}$  mice, adjusted  $p < 0.001$  compared to regular diet).  
306 Aldosterone on the high  $K^+$  diet was higher in  $\gamma^{mt/mt}$  mice (\*  $p = 0.01$ , as determined by Student's t-test,  
307 adjusted for multiple comparisons using Sidak's multiple comparisons test.) Please see Table 2 for  
308 analysis by sex.

309 **Figure 7. Body composition analysis reveals no significant difference in body water, lean tissue mass,**  
310 **or fat mass on a regular diet, but shows differences of body water and lean tissue mass to in response**  
311 **to a low or high salt diet.** Body composition in 129sv mice was measured using quantitative magnetic  
312 resonance. Circles represent female mice, squares represent males. Starting weights were similar  
313 between groups. Prior to dietary manipulation, as a percentage of total body weight, there were no  
314 differences in body composition. These animals were placed on a  $Na^+$ -depleted (0.01-0.02%  $Na^+$ ) diet,  
315 and subsequent body composition variables were normalized to baseline for each animal. Triangles and  
316 diamonds represent  $\gamma^{mt/mt}$  and  $\gamma^{+/+}$  mice, respectively. Weight declined but did not differ between  
317 genotypes. At day 2, normalized body water was lower in  $\gamma^{mt/mt}$  mice than in  $\gamma^{+/+}$  mice ( $p = 0.03$ ), and  
318 normalized lean tissue mass was lower in  $\gamma^{mt/mt}$  mice ( $p < 0.01$ ). Normalized fat content did not differ

319 between  $\gamma^{+/+}$  and  $\gamma^{mt/mt}$  mice. Composition did not differ on subsequent days. After a 10 day recovery on  
320 regular diet, effect of 2% saline on body composition was evaluated. 2% saline increased weights  
321 overall, but genotypes did not differ. On day 2, normalized body water and lean tissue increased in  
322  $\gamma^{mt/mt}$  mice compared to controls ( $p = 0.03$  and  $p = 0.04$ , respectively). Thereafter, composition did not  
323 differ between genotypes. Body fat increased similarly in  $\gamma^{+/+}$  and  $\gamma^{mt/mt}$  mice. Baseline differences  
324 between genotypes were assessed by two-tailed t-test. Changes in body composition following dietary  
325 changes were analyzed using two-way ANOVA ( $\dagger$ :  $p < 0.05$ ,  $\ddagger$ :  $p < 0.01$ ,  $\dagger\dagger\dagger$ :  $p < 0.0001$  for time as a source  
326 of variation). Differences in genotypes over time were assessed by two-stage linear step-up procedure  
327 of Benjamini, Krieger and Yekutieli (\*:  $p < 0.05$ . \*\*:  $p < 0.01$ ).

328

329

330 **REFERENCES**

- 331 1. **Bagchi RA, Ferguson BS, Stratton MS, Hu T, Cavasin MA, Sun L, Lin YH, Liu D, Londono P, Song**  
332 **K, Pino MF, Sparks LM, Smith SR, Scherer PE, Collins S, Seto E, and McKinsey TA.** HDAC11 suppresses  
333 the thermogenic program of adipose tissue via BRD2. *JCI insight* 3: 2018.
- 334 2. **Barker PM, Nguyen MS, Gatzky JT, Grubb B, Norman H, Hummler E, Rossier B, Boucher RC, and**  
335 **Koller B.** Role of gammaENaC subunit in lung liquid clearance and electrolyte balance in newborn mice.  
336 Insights into perinatal adaptation and pseudohypoaldosteronism. *The Journal of clinical investigation*  
337 102: 1634-1640, 1998.
- 338 3. **Benjamini Y, Krieger AM, and Yekutieli D.** Adaptive linear step-up procedures that control the  
339 false discovery rate. *Biometrika* 93: 491-507, 2006.
- 340 4. **Boscardin E, Perrier R, Sergi C, Maillard M, Loffing J, Loffing-Cueni D, Koesters R, Rossier BC,**  
341 **and Hummler E.** Severe hyperkalemia is rescued by low-potassium diet in renal  $\beta$ ENaC-deficient mice.  
342 *Pflügers Archiv-European Journal of Physiology* 469: 1387-1399, 2017.
- 343 5. **Boscardin E, Perrier R, Sergi C, Maillard MP, Loffing J, Loffing-Cueni D, Koesters R, Rossier BC,**  
344 **and Hummler E.** Plasma potassium determines NCC abundance in adult kidney-specific  $\gamma$ ENaC knockout.  
345 *Journal of the American Society of Nephrology* 29: 977-990, 2018.
- 346 6. **Boyd-Shiwarski CR, Weaver CJ, Beacham RT, Shiwarski DJ, Connolly KA, Nkashama LJ,**  
347 **Mutchler SM, Griffiths SE, Knoell SA, and Sebastiani RS.** Effects of extreme potassium stress on blood  
348 pressure and renal tubular sodium transport. *American Journal of Physiology-Renal Physiology* 318:  
349 F1341-F1356, 2020.



- 350 7. **Carrisoza-Gaytan R, Ray EC, Flores D, Marciszyn AL, Wu P, Liu L, Subramanya AR, Wang W,**  
351 **Sheng S, Nkashama LJ, Chen J, Jackson EK, Mutchler SM, Heja S, Kohan DE, Satlin LM, and Kleyman TR.**  
352 Intercalated cell BK $\alpha$  subunit is required for flow-induced K<sup>+</sup> secretion. *JCI insight* 5: 2020.
- 353 8. **Chung W-S, Weissman JL, Farley J, and Drummond HA.**  $\beta$ ENaC is required for whole cell  
354 mechanically gated currents in renal vascular smooth muscle cells. *American Journal of Physiology-Renal*  
355 *Physiology* 304: F1428-F1437, 2013.
- 356 9. **Drummond HA, Grifoni SC, Abu-Zaid A, Gousset M, Chiposi R, Barnard JM, Murphey B, and**  
357 **Stec DE.** Renal inflammation and elevated blood pressure in a mouse model of reduced  $\beta$ -ENaC.  
358 *American Journal of Physiology-Renal Physiology* 301: F443-F449, 2011.
- 359 10. **Drummond HA, Price MP, Welsh MJ, and Abboud FM.** A molecular component of the arterial  
360 baroreceptor mechanotransducer. *Neuron* 21: 1435-1441, 1998.
- 361 11. **Drummond HA, and Stec DE.**  $\beta$ ENaC acts as a mechanosensor in renal vascular smooth muscle  
362 cells that contributes to renal myogenic blood flow regulation, protection from renal injury and  
363 hypertension. *Journal of nephrology research* 1: 1-9, 2015.
- 364 12. **Flurkey K, and Curren JM.** *The Jackson Laboratory handbook on genetically standardized mice.*  
365 Jackson Laboratory, 2009.
- 366 13. **Frindt G, and Palmer LG.** K<sup>+</sup> secretion in the rat kidney: Na<sup>+</sup> channel-dependent and -  
367 independent mechanisms. *American journal of physiology Renal physiology* 297: F389-396, 2009.
- 368 14. **Grifoni SC, Chiposi R, McKey SE, Ryan MJ, and Drummond HA.** Altered whole kidney blood flow  
369 autoregulation in a mouse model of reduced beta-ENaC. *American journal of physiology Renal*  
370 *physiology* 298: F285-292, 2010.

- 371 15. **Hall JE, and Hall ME.** *Guyton and Hall textbook of medical physiology e-Book*. Elsevier Health  
372 Sciences, 2020.
- 373 16. **Hummler E.** Epithelial sodium channel, salt intake, and hypertension. *Current hypertension*  
374 *reports* 5: 11-18, 2003.
- 375 17. **Hummler E, Barker P, Gatzky J, Beermann F, Verdumo C, Schmidt A, Boucher R, and Rossier BC.**  
376 Early death due to defective neonatal lung liquid clearance in alpha-ENaC-deficient mice. *Nat Genet* 12:  
377 325-328, 1996.
- 378 18. **Kim J-Y, van de Wall E, Laplante M, Azzara A, Trujillo ME, Hofmann SM, Schraw T, Durand JL, Li**  
379 **H, Li G, Jelicks LA, Mehler MF, Hui DY, Deshaies Y, Shulman GI, Schwartz GJ, and Scherer PE.** Obesity-  
380 associated improvements in metabolic profile through expansion of adipose tissue. *The Journal of*  
381 *clinical investigation* 117: 2621-2637, 2007.
- 382 19. **Kinsman B, Cowles J, Lay J, Simmonds SS, Browning KN, and Stocker SD.** Osmoregulatory thirst  
383 in mice lacking the transient receptor potential vanilloid type 1 (TRPV1) and/or type 4 (TRPV4) receptor.  
384 *American Journal of Physiology-Regulatory, Integrative and Comparative Physiology* 307: R1092-R1100,  
385 2014.
- 386 20. **Kitada K, Daub S, Zhang Y, Klein JD, Nakano D, Pedchenko T, Lantier L, LaRocque LM, Marton**  
387 **A, and Neubert P.** High salt intake reprioritizes osmolyte and energy metabolism for body fluid  
388 conservation. *The Journal of clinical investigation* 127: 1944-1959, 2017.
- 389 21. **Malnic G, Giebisch G, Muto S, Wang W, Bailey MA, and Satlin LM.** Regulation of K<sup>+</sup> excretion.  
390 In: *Seldin and Giebisch's The Kidney* Elsevier, 2013, p. 1659-1715.

- 391 22. **McDonald FJ, Yang B, Hrstka RF, Drummond HA, Tarr DE, McCray PB, Jr., Stokes JB, Welsh MJ,**  
392 **and Williamson RA.** Disruption of the beta subunit of the epithelial Na<sup>+</sup> channel in mice: hyperkalemia  
393 and neonatal death associated with a pseudohypoaldosteronism phenotype. *Proceedings of the*  
394 *National Academy of Sciences of the United States of America* 96: 1727-1731, 1999.
- 395 23. **Miller RL, Wang MH, Gray PA, Salkoff LB, and Loewy AD.** ENaC-expressing neurons in the  
396 sensory circumventricular organs become c-Fos activated following systemic sodium changes. *American*  
397 *Journal of Physiology-Regulatory, Integrative and Comparative Physiology* 305: R1141-R1152, 2013.
- 398 24. **Morla L, Shore O, Lynch IJ, Merritt ME, and Wingo CS.** A non-invasive method to study  
399 evolution of extracellular fluid volume in mice using time domain nuclear magnetic resonance. *American*  
400 *Journal of Physiology-Renal Physiology* 2020.
- 401 25. **Pavlov TS, and Staruschenko A.** Involvement of ENaC in the development of salt-sensitive  
402 hypertension. *American Journal of Physiology-Renal Physiology* 313: F135-F140, 2017.
- 403 26. **Perrier R, Boscardin E, Malsure S, Sergi C, Maillard MP, Loffing J, Loffing-Cueni D, Sørensen**  
404 **MV, Koesters R, and Rossier BC.** Severe salt-losing syndrome and hyperkalemia induced by adult  
405 nephron-specific knockout of the epithelial sodium channel  $\alpha$ -subunit. *Journal of the American Society*  
406 *of Nephrology* 27: 2309-2318, 2016.
- 407 27. **Pham CT, MacIvor DM, Hug BA, Heusel JW, and Ley TJ.** Long-range disruption of gene  
408 expression by a selectable marker cassette. *Proceedings of the National Academy of Sciences of the*  
409 *United States of America* 93: 13090-13095, 1996.
- 410 28. **Pitzer AL, Van Beusecum JP, Kleyman TR, and Kirabo A.** ENaC in Salt-Sensitive Hypertension:  
411 Kidney and Beyond. *Current Hypertension Reports* 22: 69, 2020.

- 412 29. **Pradervand S, Barker PM, Wang Q, Ernst SA, Beermann F, Grubb BR, Burnier M, Schmidt A,**  
413 **Bindels RJ, Gatzky JT, Rossier BC, and Hummler E.** Salt restriction induces pseudohypoaldosteronism  
414 type 1 in mice expressing low levels of the beta-subunit of the amiloride-sensitive epithelial sodium  
415 channel. *Proceedings of the National Academy of Sciences of the United States of America* 96: 1732-  
416 1737, 1999.
- 417 30. **Rakova N, Juttner K, Dahlmann A, Schroder A, Linz P, Kopp C, Rauh M, Goller U, Beck L,**  
418 **Agureev A, Vassilieva G, Lenkova L, Johannes B, Wabel P, Moissl U, Vienken J, Gerzer R, Eckardt KU,**  
419 **Muller DN, Kirsch K, Morukov B, Luft FC, and Titze J.** Long-term space flight simulation reveals infradian  
420 rhythmicity in human Na(+) balance. *Cell Metab* 17: 125-131, 2013.
- 421 31. **Randrianarison N, Clerici C, Ferreira C, Fontayne A, Pradervand S, Fowler-Jaeger N, Hummler E,**  
422 **Rossier BC, and Planes C.** Low expression of the beta-ENaC subunit impairs lung fluid clearance in the  
423 mouse. *Am J Physiol Lung Cell Mol Physiol* 294: L409-416, 2008.
- 424 32. **Ray EC.** ENaC blockade in proteinuria-associated extracellular fluid volume overload - effective  
425 but risky. *Physiol Rep* 6: e13835, 2018.
- 426 33. **Ray EC, Carrisoza-Gaytan R, Al-Bataineh M, Marciszyn A, Nkashama LJ, Chen J, Winfrey A,**  
427 **Flores D, Wu P, Wang W, Huang CL, Subramanya AR, Kleyman TR, and Satlin LM.** L-WNK1 is required  
428 for BK channel activation in intercalated cells. *AJP-Renal Physiol*, under review 2020.
- 429 34. **Ray EC, Chen J, Kelly TN, He J, Hamm LL, Gu D, Shimmin LC, Hixson JE, Rao DC, Sheng S, and**  
430 **Kleyman TR.** Human epithelial Na<sup>+</sup> channel missense variants identified in the GenSalt study alter  
431 channel activity. *American journal of physiology Renal physiology* 311: F908-f914, 2016.

- 432 35. **Ray EC, Rondon-Berrios H, Boyd CR, and Kleyman TR.** Sodium retention and volume expansion  
433 in nephrotic syndrome: implications for hypertension. *Advances in chronic kidney disease* 22: 179-184,  
434 2015.
- 435 36. **Rubera I, Loffing J, Palmer LG, Frindt G, Fowler-Jaeger N, Sauter D, Carroll T, McMahon A,**  
436 **Hummler E, and Rossier BC.** Collecting duct-specific gene inactivation of  $\alpha$ ENaC in the mouse kidney  
437 does not impair sodium and potassium balance. *The Journal of clinical investigation* 112: 554-565, 2003.
- 438 37. **Schild L.** The ENaC channel as the primary determinant of two human diseases: Liddle syndrome  
439 and pseudohypoaldosteronism. *Nephrologie* 17: 395-400, 1996.
- 440 38. **Šidák Z.** Rectangular Confidence Regions for the Means of Multivariate Normal Distributions.  
441 *Journal of the American Statistical Association* 62: 626-633, 1967.
- 442 39. **Snyder PM.** The epithelial Na<sup>+</sup> channel: cell surface insertion and retrieval in Na<sup>+</sup> homeostasis  
443 and hypertension. *Endocr Rev* 23: 258-275, 2002.
- 444 40. **Taicher GZ, Tinsley FC, Reiderman A, and Heiman ML.** Quantitative magnetic resonance (QMR)  
445 method for bone and whole-body-composition analysis. *Analytical and bioanalytical chemistry* 377: 990-  
446 1002, 2003.
- 447 41. **Tarjus A, Maase M, Jeggle P, Martinez-Martinez E, Fassot C, Loufrani L, Henrion D, Hansen PB,**  
448 **Kusche-Vihrog K, and Jaisser F.** The endothelial  $\alpha$ ENaC contributes to vascular endothelial function in  
449 vivo. *PloS one* 12: e0185319, 2017.
- 450 42. **Theander-Carrillo C, Wiedmer P, Cettour-Rose P, Nogueiras R, Perez-Tilve D, Pfluger P,**  
451 **Castaneda TR, Muzzin P, Schürmann A, Szanto I, Tschöp MH, and Rohner-Jeanrenaud F.** Ghrelin action  
452 in the brain controls adipocyte metabolism. *The Journal of clinical investigation* 116: 1983-1993, 2006.

- 453 43. **Tinsley FC, Taicher GZ, and Heiman ML.** Evaluation of a Quantitative Magnetic Resonance  
454 Method for Mouse Whole Body Composition Analysis. *Obesity Research* 12: 150-160, 2004.
- 455 44. **Unruh ML, Pankratz MS, Demko JE, Ray EC, Hughey RP, and Kleyman TR.** Trial of Amiloride in  
456 Type 2 Diabetes with Proteinuria. *Kidney Int Rep In press*, 2017.
- 457

**Table 2. Blood measurements on a high K<sup>+</sup> diet.**

	$\gamma^{+/+}$	$\gamma^{mt/mt}$	Male $\gamma^{+/+}$	Male $\gamma^{mt/mt}$	Female $\gamma^{+/+}$	Female $\gamma^{mt/mt}$
Na <sup>+</sup> (mmol/L)	147 ± 2 (19)	147 ± 3 (24)	147 ± 2 (10)	148 ± 2 (17)	146 ± 2 (9)	144 ± 2 (7)*
K <sup>+</sup> (mmol/L)	5.2 ± 0.6 (19)	5.4 ± 0.7 (24)	5.0 ± 0.7 (10)	5.5 ± 0.7 (17)	5.5 ± 0.5 (9)	5.2 ± 0.7 (7)
Cl <sup>-</sup> (mmol/L)	119 ± 3 (19)	119 ± 3 (23)	118 ± 3 (10)	119 ± 3 (16)	119 ± 4 (9)	119 ± 4 (7)
tCO <sub>2</sub> (mmol/L)	20 ± 2 (19)	20 ± 2 (24)	21 ± 2 (10)	21 ± 1 (17)	20 ± 2 (9)	18 ± 2 (7)
Urea nitrogen (mg/dL)	26 ± 4 (19)	28 ± 4 (24)	28 ± 4 (10)	28 ± 4 (17)	25 ± 3 (9)	29 ± 6 (7)
Hemoglobin (mg/dL)	13.3 ± 0.9 (19)	13.5 ± 0.9 (24)	13.4 ± 0.7 (10)	13.6 ± 0.8 (17)	13.2 ± 1.1 (9)	13.4 ± 1 (7)
Creatinine (mg/dL)	< 0.2 md/dL	< 0.2 md/dL	< 0.2 md/dL	< 0.2 md/dL	< 0.2 md/dL	< 0.2 md/dL
Aldosterone (pg/mL)	3100 ± 2500 (19)	4900 ± 2500 (23)*	3100 ± 2800 (10)	4600 ± 2500 (17)	3000 ± 2200 (9)	5800 ± 2700 (6)

Animals were given high K<sup>+</sup> diet (5.2% K<sup>+</sup>, as KCl) for 10 days. Electrolytes, urea nitrogen, hemoglobin, and creatinine were assayed in whole blood. Creatinine values were all below the detection threshold. Aldosterone was measured in plasma. Differences were assessed using a two-tailed Student's t-test, with adjustment of *p* values for multiple comparisons (two sexes) using Sidak's method. \*: *p* < 0.05 for difference between  $\gamma^{+/+}$  and  $\gamma^{-/-}$ .

**Table 1. Blood measurements on a regular diet**

	$\gamma^{+/+}$	$\gamma^{mt/mt}$	Male $\gamma^{+/+}$	Male $\gamma^{mt/mt}$	Female $\gamma^{+/+}$	Female $\gamma^{mt/mt}$
Na <sup>+</sup> (mmol/L)	145 ± 2 (21)	144 ± 2 (16)	145 ± 1 (13)	145 ± 2 (10)	144 ± 2 (8)	143 ± 1 (6)
K <sup>+</sup> (mmol/L)	4.9 ± 0.7 (20)	4.9 ± 0.6 (16)	5.0 ± 0.7 (12)	4.9 ± 0.4 (10)	4.7 ± 0.7 (8)	4.8 ± 0.8 (6)
Cl <sup>-</sup> (mmol/L)	113 ± 2 (14)	113 ± 3 (16)	113 ± 2 (9)	113 ± 2 (10)	114 ± 2 (5)	112 ± 3 (6)
tCO <sub>2</sub> (mmol/L)	24.8 ± 3.3 (20)	24.5 ± 2.3 (16)	26.5 ± 3.1 (12)	25.2 ± 1.6 (10)	22.3 ± 1.7 (8)	23.3 ± 2.9 (6)
Urea Nitrogen (mg/dL)	27 ± 5 (14)	28 ± 5 (16)	28 ± 5 (9)	28 ± 5 (10)	25 ± 5.5 (5)	27 ± 6 (6)
Hemoglobin (mg/dL)	13.1 ± 0.9 (20)	13.6 ± 0.8 (16)	13.3 ± 0.5 (12)	13.5 ± 0.8 (10)	12.9 ± 1.3 (8)	13.8 ± 1.0 (6)
Creatinine (mg/dL)	< 0.2 md/dL	< 0.2 md/dL	< 0.2 md/dL	< 0.2 md/dL	< 0.2 md/dL	< 0.2 md/dL
Aldosterone (pg/mL)	590 ± 720 (11)	880 ± 610 (9)	420 ± 290 (8)	880 ± 580 (5)	1040 ± 1380 (3)	890 ± 750 (4)
ANP (pg/mL)	221 ± 114 (11)	191 ± 101 (10)	259 ± 112 (8)	227 ± 104 (6)	121 ± 11 (3)	136 ± 77 (4)

Blood parameters from mice on a regular diet are shown: mean ± standard deviation (N). Electrolytes, urea nitrogen, hemoglobin, and creatinine were assayed in whole blood. All creatinine values were below the detection threshold. Aldosterone and atrial natriuretic peptide (ANP) measurements were measured in plasma. There were no significant differences between  $\gamma^{+/+}$  mice and  $\gamma^{mt/mt}$  mice, either in male mice or female mice, or when mice from both sexes were pooled, as determined by two-tailed Student's t-test with adjustment of *p* values for multiple comparisons (two sexes) using Sidak's method.



**Figure 1.**

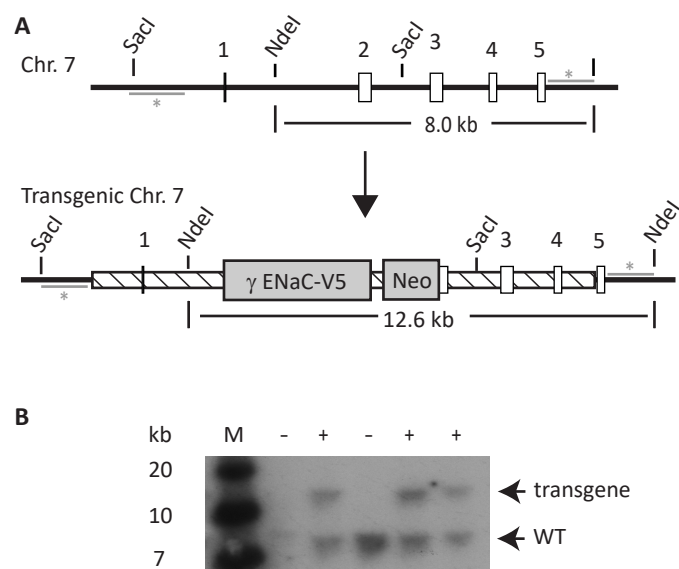
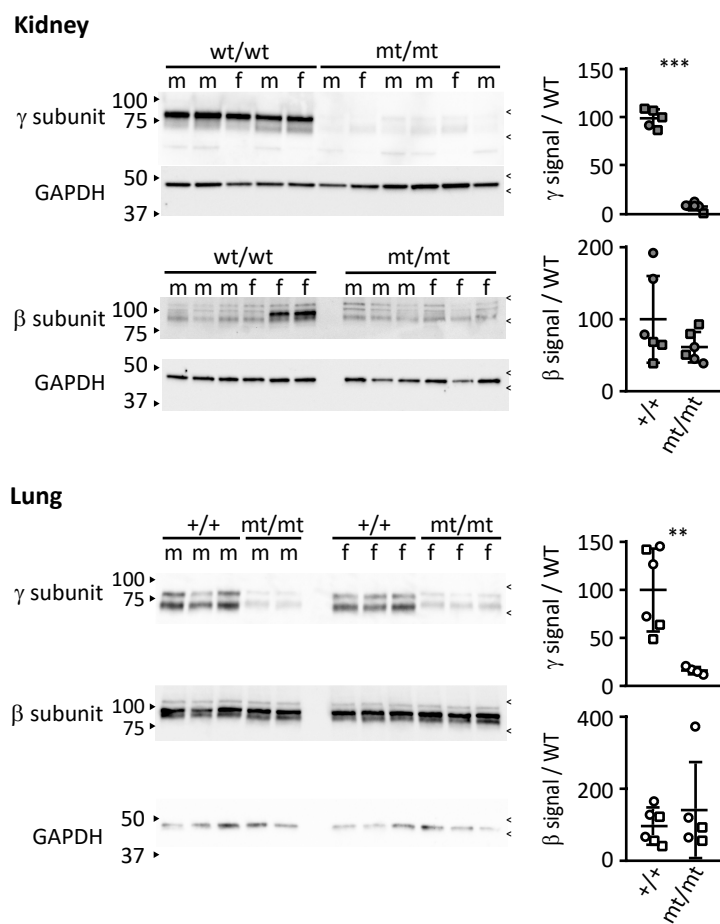


Figure 2.



**Figure 3.**

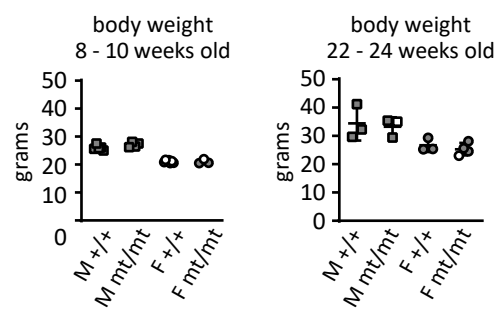


Figure 4.

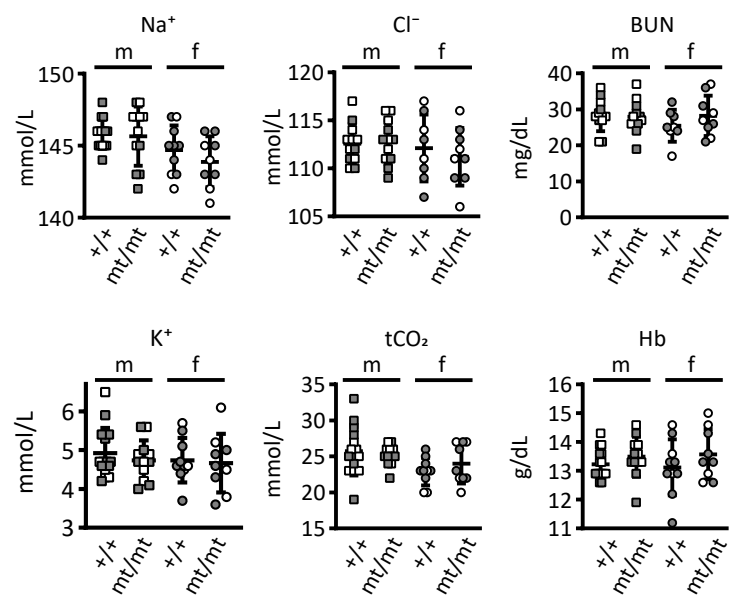
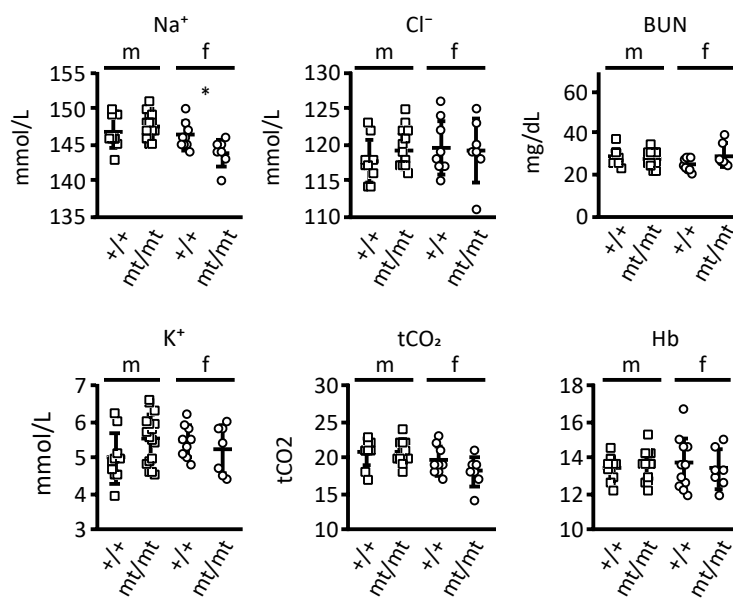


Figure 5.



**Figure 6.**

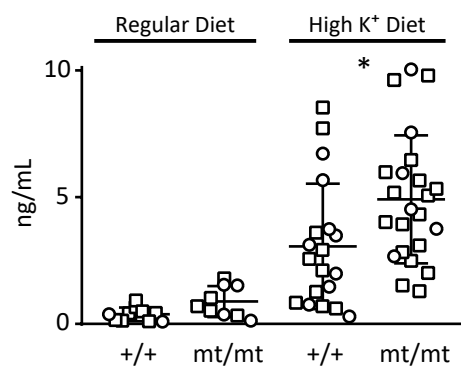


Figure 7.

